World Journal of Engineering Research
Print ISSN: 2959-9865
Online ISSN: 2959-9873
DOI: https://doi.org/10.61784/wjer3079

HYBRID-CONTROLLED IPOS LLC CONVERTER FOR FUEL CELL APPLICATIONS

JueXiao Chen[1], EnYong Li[1], Lei Shi[1*], ZhongYao Jiang[2*]
[1]*School of Automotive and Energy Studies, Tongji University, Shanghai 201804, China.*
[2]*Jiangsu Qunling Energy Technology Co., Ltd, Nantong 226407, Jiangsu, China.*
[*]*Lei Shi and ZhongYao Jiang contribute the same to the article and are the corresponding authors.*
[*]*Corresponding Author: Lei Shi, ZhongYao Jiang*

Abstract: Fuel-cell power conditioning systems require DC–DC converters to achieve high efficiency, wide-range voltage regulation, and reliable operation under significant input and load variations. To address these requirements, this paper investigates an IPOS-type secondary LLC resonant DC–DC converter and proposes a hybrid control strategy combining pulse-frequency modulation (PFM) and phase-shift modulation (PSM). In the proposed scheme, PFM is employed as the primary control method to realize wide-range voltage regulation, while a frequency-clamping with phase-shift compensation mechanism is introduced to maintain effective power control and dynamic performance when the switching frequency reaches its practical upper limit. The effectiveness of the proposed topology and control strategy is validated through MATLAB/Simulink simulations and experimental studies on a laboratory prototype. Experimental results demonstrate a peak conversion efficiency of 96.6% under rated conditions, with efficiency remaining above 96% near the rated load range. In addition, the maximum output voltage deviation between two IPOS phases is limited to 1.9% under full-load operation, and fast, stable input-current tracking is achieved under step reference changes from 20 A to 80 A without noticeable overshoot. These results confirm that the proposed converter and hybrid control strategy are well suited for high-efficiency, wide-range fuel-cell energy conversion applications.
Keywords: Fuel cell system; LLC resonant converter; Hybrid control

1 INTRODUCTION

Fuel cells are increasingly regarded as a key enabling technology for sustainable energy systems owing to their high efficiency, low emissions, and scalability in transportation, stationary, and portable power applications. Nevertheless, the inherent variability of fuel-cell output voltage and load conditions imposes stringent requirements on DC–DC converters to maintain high efficiency and stable regulation over a wide operating range [1-2]. In high-power applications such as electric vehicles and renewable-energy grid integration, the converter must further satisfy demanding constraints on safety, reliability, and power density.

DC–DC converters for fuel-cell conditioning can be generally categorized into non-isolated and isolated topologies. Non-isolated converters are attractive for low- to medium-power systems due to their compact structure, low cost, and simple control [3-4], but their limited voltage conversion ratio and the lack of galvanic isolation raise safety concerns in high-voltage applications [5-6]. Isolated converters, enabled by high-frequency transformers, provide galvanic isolation and are therefore more suitable for high-gain and high-power scenarios [7]. With continuous progress in high-frequency switching and magnetic-component design, isolated converters have achieved improved power density, making them a practical choice for fuel-cell-based systems that may also require bidirectional power flow for G2V/V2G operation [8-9].

Among isolated solutions, the LLC resonant converter is widely adopted due to its high efficiency, soft-switching capability (ZVS/ZCS), and low EMI [10]. However, conventional LLC designs often suffer from noticeable efficiency degradation when the required voltage-gain regulation range exceeds approximately 1.5×, which limits their applicability in wide-range operation [11]. To extend the regulation range, prior studies have investigated topology-level enhancements (e.g., coupled-inductor integration and adaptive-frequency techniques) and integrated/multiport resonant structures with switch multiplexing to suppress switching-frequency excursion and reduce component count [12-13]. In addition, hybrid modulation strategies combining PFM with PSM or PWM have been reported to improve regulation flexibility while maintaining high efficiency across a wider voltage range [14-15]. Despite these advances, a key remaining challenge is that the converter may encounter a constrained switching-frequency window in practical high-power designs (due to device limitations, magnetic design, and efficiency considerations), where pure PFM alone becomes insufficient for power regulation and dynamic performance.

For high-voltage-gain and high-power-density requirements, the IPOS LLC architecture provides a modular approach by connecting multiple LLC sub-modules in series at the output while paralleling the input, thereby enabling scalable voltage boosting and reduced input current stress per module [16-17]. However, component tolerances in the resonant tank can lead to inter-module voltage/current imbalance, which degrades efficiency and reliability [18]. Although current-balancing methods such as DGR-based strategies have been proposed [19], the increased hardware complexity and magnetic-component count may raise cost and hinder volume optimization [20]. Therefore, for fuel-cell conditioning where wide-range regulation, high efficiency, and reliable operation are simultaneously required, it is of

practical interest to develop a control-oriented design framework that supports wide-range operation without excessive frequency excursion or added hardware complexity.

Motivated by the above challenges, this paper focuses on the control and experimental validation of an IPOS-type secondary LLC resonant DC–DC converter for fuel-cell power conditioning applications. A hybrid PFM–PSM modulation strategy is proposed, in which PFM is used as the primary control method to achieve wide-range voltage regulation, while PSM is introduced as an auxiliary means under switching-frequency constraints to ensure continuous power control and favorable dynamic performance. A frequency-clamping with phase-shift compensation mechanism is further developed to overcome the limitations of pure frequency modulation at high switching frequencies. The main contributions of this paper can be summarized as follows:

(1) An IPOS-type secondary LLC resonant converter suitable for wide input/output range fuel-cell applications is analyzed and implemented;

(2) A hybrid PFM–PSM control strategy with frequency-clamping and phase-shift compensation is proposed to extend the effective regulation range under practical constraints;

(3) The effectiveness of the proposed converter and control strategy is experimentally demonstrated, achieving high efficiency, good output voltage balancing, and fast dynamic response.

The remainder of this paper is organized as follows. Section II describes the topology and operating principles of the proposed converter. Section III presents the steady-state characteristics and introduces the hybrid control strategy and its operating mechanisms. Simulation and experimental results are provided in Section IV, and conclusions are drawn in Section V.

2 TOPOLOGY AND OPERATING PRINCIPLE

2.1 Operating Principle Under PFM Operation

As illustrated in Figure 1, the IPOS-type secondary LLC resonant converter consists of an inverter stage, a resonant network, and a rectification stage. The rectification stage is composed of four rectifier diodes, which are responsible for converting the high-frequency AC voltage into a DC output. The inverter stage comprises a DC input source and two half-bridge legs, generating a high-frequency square-wave voltage that is transferred to the resonant network through a high-frequency transformer. The resonant network is formed by the resonant inductor, resonant capacitor, and the transformer magnetizing inductance. Owing to the series resonance between the resonant inductor and resonant capacitor, zero-voltage switching (ZVS) of the inverter-side switches and zero-current switching (ZCS) of the rectifier diodes are achieved. The processed energy is then delivered to the rectification stage to complete DC power conversion.

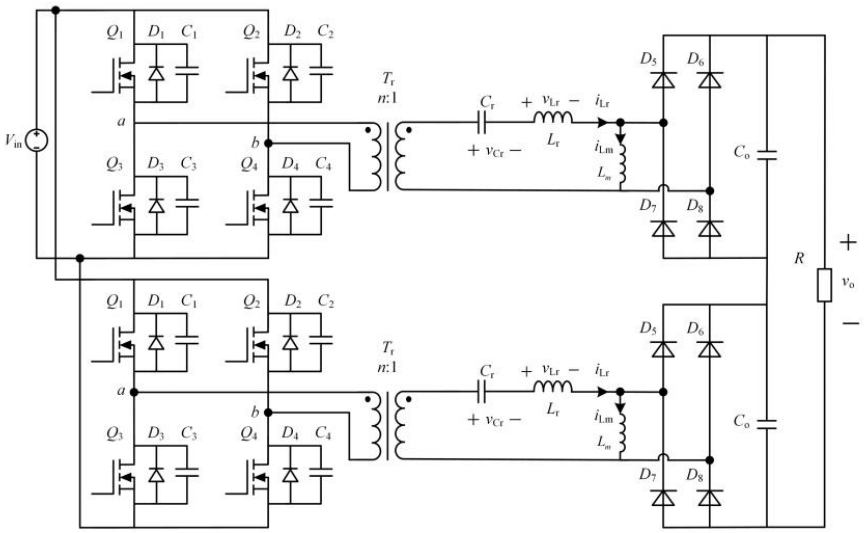

Figure 1 Circuit Diagram of the IPOS-Type Secondary LLC Resonant Converter

The voltage gain of a full-bridge LLC resonant converter is regulated by controlling the switching frequency of the inverter-stage power switches. According to the relationship among the resonant frequency, the magnetizing resonant frequency, and the actual operating switching frequency, the operating modes of the converter can be classified into three categories: the under-resonant mode($f_m < f_s < f_r$), the quasi-resonant mode($f_s = f_r$), and the over-resonant mode($f_s > f_r$). To achieve high conversion efficiency, the converter studied in this paper is designed to operate only in the under-resonant and quasi-resonant modes.

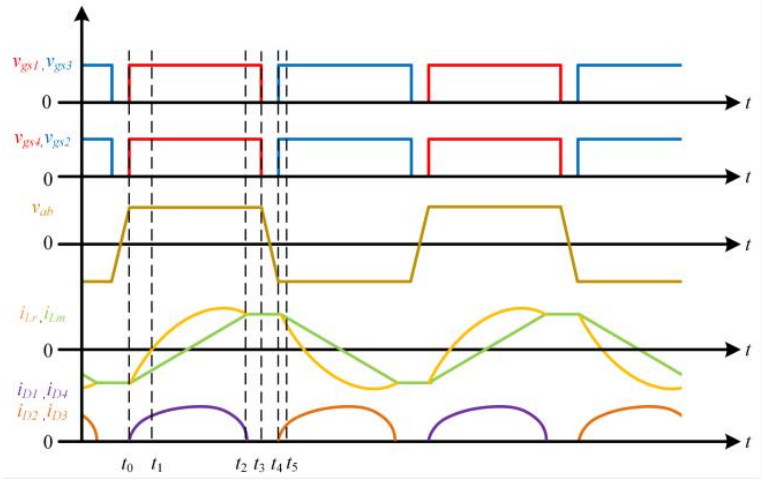

Figure 2 Operating Sequence Diagram

Figure 2 illustrates the operating waveforms of the full-bridge LLC resonant converter in the under-resonant mode. It can be observed that this mode includes both stages in which the magnetizing inductance does not participate in resonance and stages in which it does participate. In this operating mode, the boundaries between different energy-transfer stages are clearly distinguishable.

Steady-state analysis of resonant converters forms the foundation for understanding their operating characteristics and for guiding design optimization. Since most electrical quantities in the resonant tank exhibit sinusoidal or quasi-sinusoidal waveforms, conventional steady-state analysis methods for PWM converters, such as the ramp approximation method, are no longer applicable. For resonant converters, the commonly adopted analysis approaches include the fundamental harmonic approximation (FHA) and the state-space averaging (SSA) method. Among these, the fundamental harmonic approximation is one of the most widely used and relatively straightforward methods for steady-state analysis of LLC resonant converters. The core idea of the FHA is that, when the resonant converter operates under a high quality factor (Q) condition, the resonant tank exhibits strong attenuation of higher-order harmonics. Consequently, the voltages and currents within the resonant network can be assumed to be predominantly sinusoidal, and only the fundamental harmonic components are considered in the analysis.

Based on the fundamental harmonic approximation, the fundamental-frequency equivalent circuit of the secondary LLC resonant converter can be derived, as shown in Figure 3.

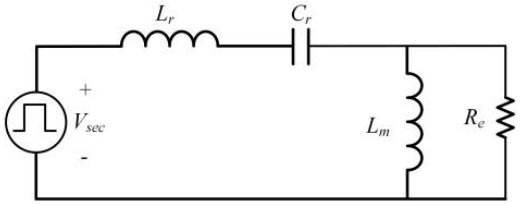

Figure 3 Fundamental Equivalent Circuit

Based on the equivalent circuit shown in Figure 3, the DC voltage gain of the resonant network in the fundamental-harmonic-approximation-based equivalent model can be derived according to Kirchhoff's voltage law (KVL) and Kirchhoff's current law (KCL) as follows:

$$M = \left|H(j\omega)\right| = \frac{1}{\sqrt{(1+\frac{1}{k}-\frac{1}{f_n^2 k})^2 + Q^2(f_n - \frac{1}{f_n})^2}} \tag{1}$$

Figure 4 depicts the DC voltage gain characteristics of the LLC resonant converter as a function of the normalized switching frequency for different quality factor (Q) values with k=4. The presented gain curves provide a useful guideline for selecting the resonant tank parameters, which can be designed according to the required maximum voltage gain of the converter.

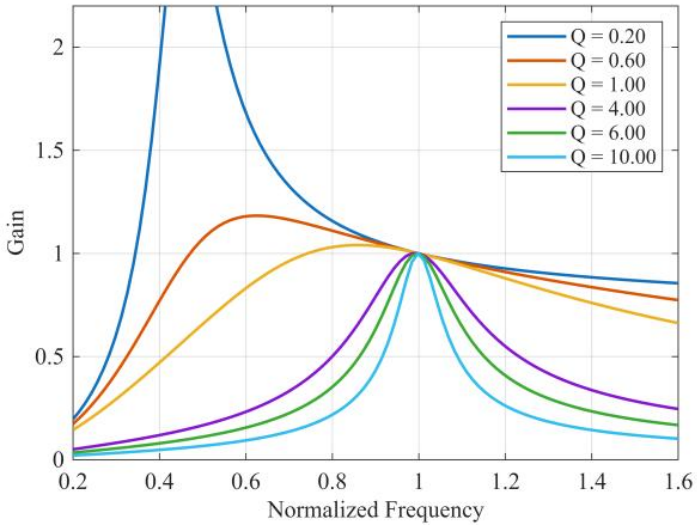

Figure 4 DC Voltage Gain Curves at Different Q Values

2.2 Operating Principle Under PSM Operation

The operating waveforms of the phase-shift modulation (PSM) scheme are illustrated in Figure 5. The signals $V_{g1} \sim V_{g4}$ represent the gate-drive signals of the converter switches $Q_1 \sim Q_4$, respectively. The gate signals V_{g1} and V_{g3} are complementary, as are V_{g2} and V_{g4}, with each pair operating at a duty cycle of 0.5. In addition, V_{g1} leads V_{g2} by a certain phase angle, and the output voltage of the inverter stage, V_{ab}, is regulated by adjusting this phase shift.

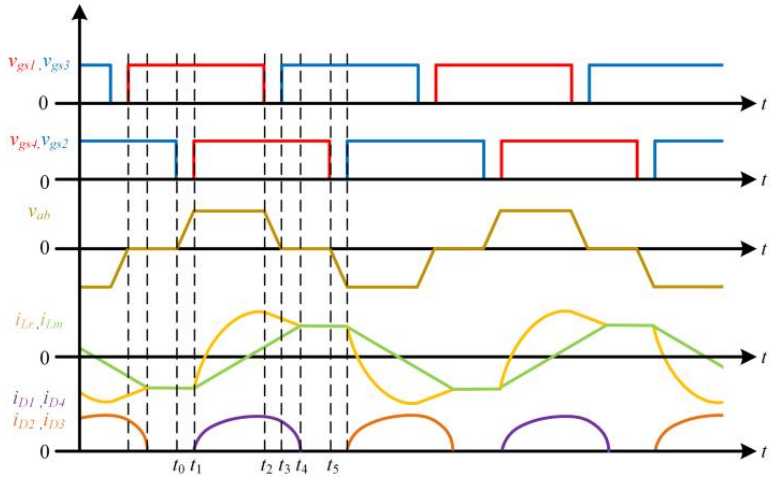

Figure 5 Operating Waveforms of the Converter Under PSM Mode

Under PSM operation, the converter operates at a fixed switching frequency, which is beneficial for the design of magnetic components. Moreover, this modulation strategy enables soft switching of both the primary-side switches and the secondary-side rectifier diodes, thereby preserving the high-efficiency characteristics of conventional LLC resonant converters typically achieved under variable-frequency control.

In the PSM mode, output voltage regulation is achieved by adjusting the phase-shift angle in response to variations in the input voltage. For PFM-controlled LLC resonant converters, voltage-gain analysis is commonly conducted using the fundamental harmonic approximation (FHA), which neglects higher-order harmonic components. However, when the LLC resonant converter operates under PSM, the contribution of higher-order harmonics in the resonant network becomes more significant. Consequently, the FHA is no longer applicable for accurate gain analysis in the PSM mode, and a time-domain analysis is required to obtain precise voltage-gain characteristics.

Based on the time-domain analysis [21-22], the relationship between the voltage gain and the effective duty ratio under PSM operation is obtained, as illustrated in Figure 6. Under phase-shift control, the resonant-tank gain of the converter is always less than or equal to unity, indicating that PSM enables only step-down operation. Accordingly, the output voltage decreases monotonically as the effective duty ratio is reduced.

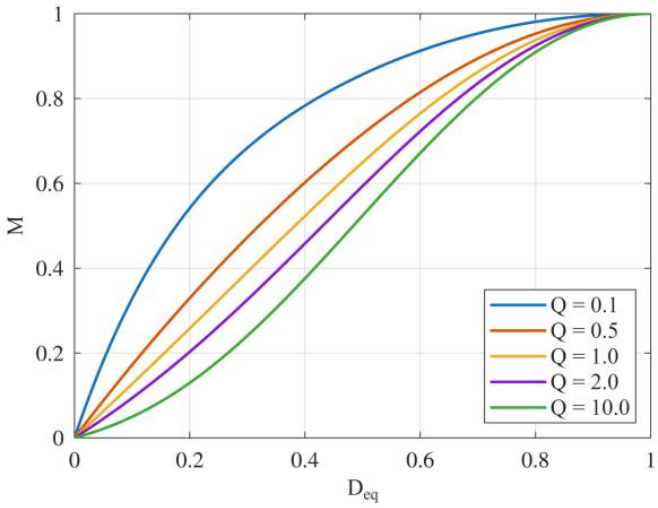

Figure 6 Voltage Gain M Versus Effective Duty Ratio D_{eq} Under PSM Mode

3 CONTROLLER DESIGN

Based on the above analysis, frequency modulation is more suitable for step-up operation, whereas phase-shift modulation is better suited for step-down operation. By exploiting the complementary advantages of these two control methods, both frequency modulation and phase-shift modulation are simultaneously applied to the full-bridge LLC resonant converter. In this paper, frequency modulation is employed as the primary control strategy, while phase-shift modulation serves as an auxiliary means, thereby forming a hybrid frequency–phase-shift modulation scheme. This control strategy not only ensures wide-range voltage regulation capability but also effectively addresses the limitations in power regulation and dynamic performance under constrained switching-frequency variation.

As illustrated in Figure 7, when the PWM period command reaches its minimum limit—corresponding to the maximum allowable switching frequency—any further increase in frequency is constrained by hardware limitations and efficiency considerations. To avoid the adverse effects associated with excessive switching frequency, the PWM period is clamped, maintaining the switching frequency at its upper permissible bound. Under this condition, phase-shift modulation is introduced as a complementary control mechanism. By adjusting the phase shift between the primary-side bridge legs, power regulation can be continuously achieved while keeping the switching frequency constant, thereby compensating for the limited regulation capability of pure frequency modulation. As a result, the system enters a "frequency-clamping with phase-shift compensation" operating region.

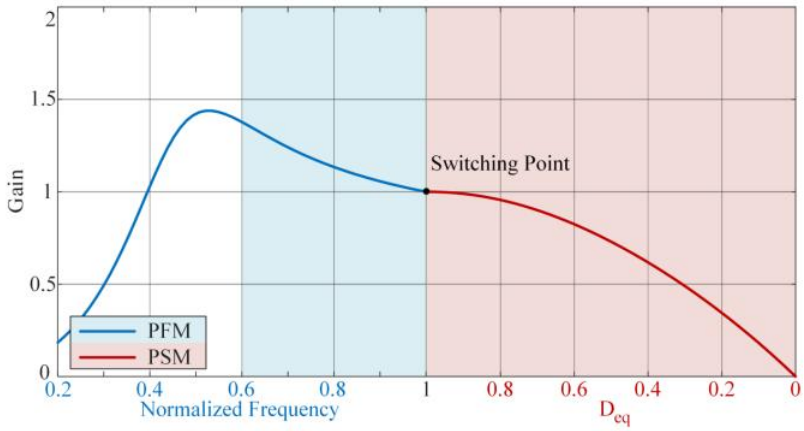

Figure 7 Hybrid Control Gain Curve and Switching Point

4 SIMULATION AND EXPERIMENT

4.1 Simulation

To verify the rationality of the resonant tank parameter design as well as the feasibility and effectiveness of the proposed control strategy, a detailed simulation model of the LLC resonant converter was established in MATLAB/Simulink, as shown in Figure 8. Based on this simulation platform, the dynamic behavior of the converter under different control schemes can be systematically evaluated (Table 1).

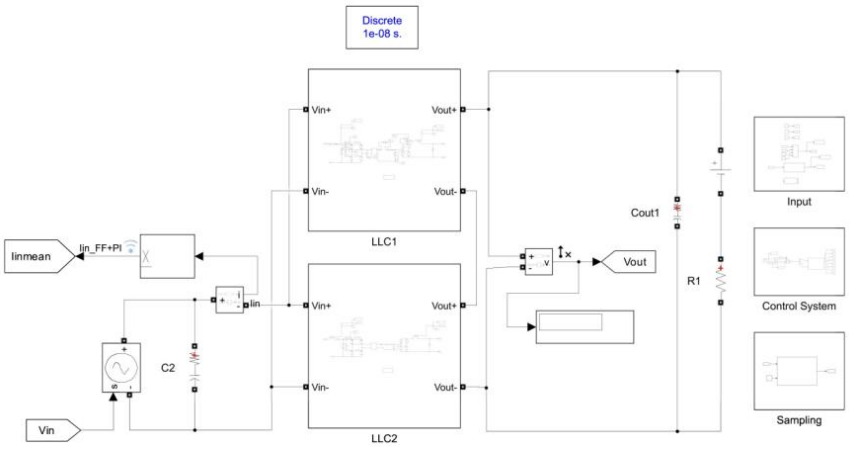

Figure 8 Topology of the IPOS-Type Secondary LLC Resonant Converter

Table 1 Parameters of the LLC Resonant Converter

Parameter	Designator	Value
Input Voltage Range	Vinmin ~ Vinmax [V]	160~280
Input Voltage Nominal	Vin [V]	200
Output Voltage Range	Vomin ~ Vomax [V]	380~560
Output Voltage Nominal	Vo [V]	460
Switching Frequency Range	Fs [kHz]	150~230
Resonant Frequency	Fr [kHz]	230
Transformer Ratio	n	0.75
Resonant Inductor	Lr [uH]	1.65
Resonant Capacitor	Cr [nF]	300
Excitation Inductor	Lm [uH]	6.6
Filter Capacitor	Co [uF]	20
Load Resistor	Ro [Ω]	6.25

To verify the rationality of the parameter design, simulations of soft switching and resonant current in the system were first performed. The obtained waveforms are shown in Figure 9.

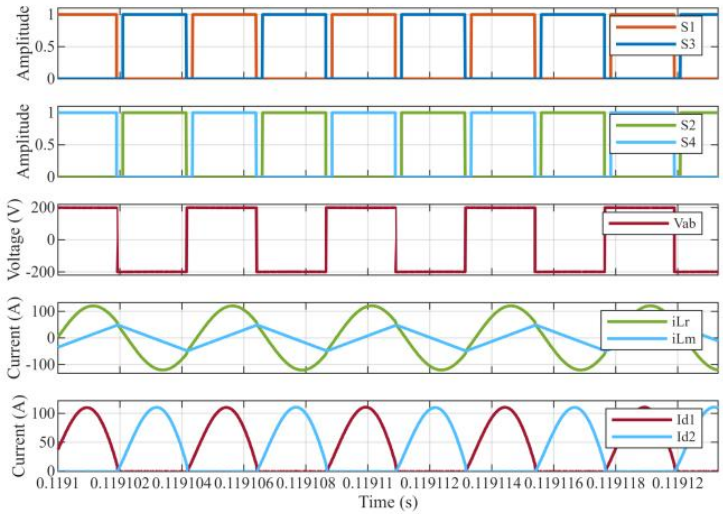

Figure 9 Simulation Waveforms of Soft Switching in the Resonant State

In the simulation shown in Figure 9, the converter operates in frequency modulation (PFM) mode, with no phase shift between the two bridge arms in the same inverter network. Analysis of the simulation waveforms reveals that the resonant current i_{Lr} and the excitation current i_{Lm} intersect at a certain point, indicating that the converter operates in a resonant state during this period. Additionally, it is observed that the switching tube trigger signals V_{gs1} and V_{gs2} are output complementarily with a certain dead time. Before switch $S2$ is turned on, its drain-source voltage V_{ds2} decreases to zero, thereby achieving the soft switching function and verifying the rationality of the system parameters designed in this study.

The simulation waveforms of the converter operating in the phase-shifted PSM mode are shown in Figure 10. Compared to the PFM mode, a certain phase difference exists between the two bridge arms, resulting in a zero-voltage interval in V_{ab} .

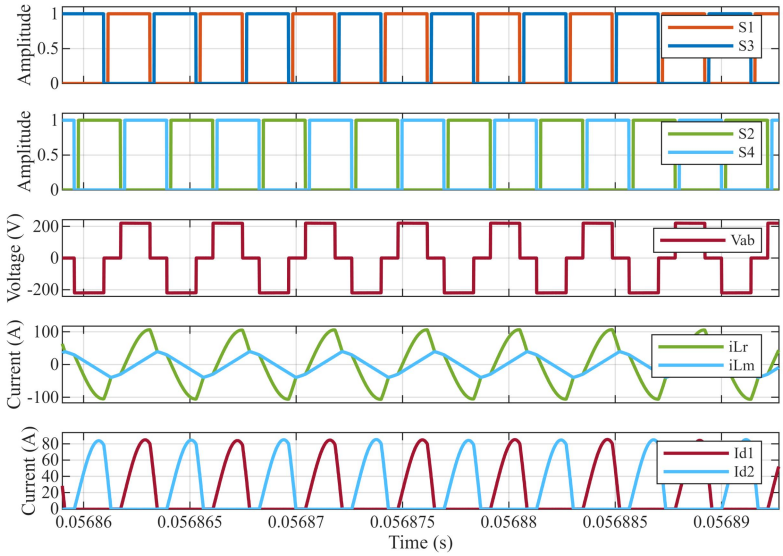

Figure 10 Simulation Waveforms of the Converter in Phase-shifted PSM mode

4.2 Experimental Verification

Figure 10 illustrates the experimental platform established to evaluate the performance of the proposed IPOS-type secondary LLC resonant DC/DC converter. The platform consists of a programmable DC power source, an experimental DC/DC converter prototype, an electronic load, a cooling system, and measurement and control equipment.

A programmable DC source is used to emulate the fuel cell output characteristics and provide a stable input voltage to the converter. The output side of the converter is connected to an electronic load, which allows flexible adjustment of load conditions for steady-state and dynamic tests. To ensure safe and reliable operation under high-power conditions, a water-cooling system is employed, with a cooling water tank supplying temperature-controlled coolant to the power module.

The converter is monitored and controlled by a host PC through a CAN communication interface, enabling real-time parameter configuration, reference command adjustment, and data acquisition. Electrical measurements are performed using a digital oscilloscope and a power analyzer. Current probes and high-voltage probes are used to accurately capture current and voltage waveforms at critical points of the converter. Through the coordinated operation of the power supply, load, cooling, control, and measurement subsystems, the experimental platform enables comprehensive evaluation of the converter's steady-state performance, dynamic response, efficiency, and voltage-balancing characteristics (Figure 11).

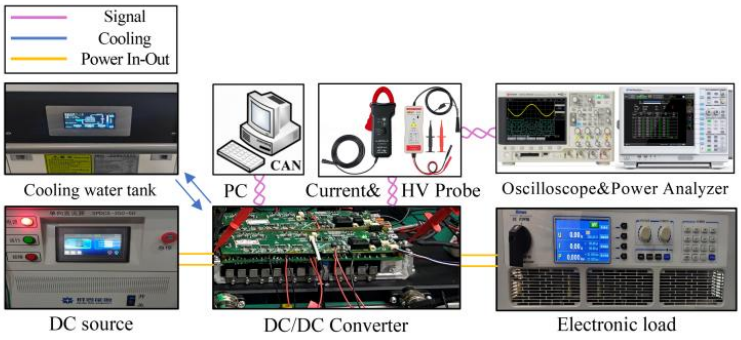

Figure 11 Experimental Platform of the LLC Resonant Converter

First, the DC adjustable power supply is set to stably output a 500 V DC voltage. The experimental results of soft switching are shown in Figure 12.

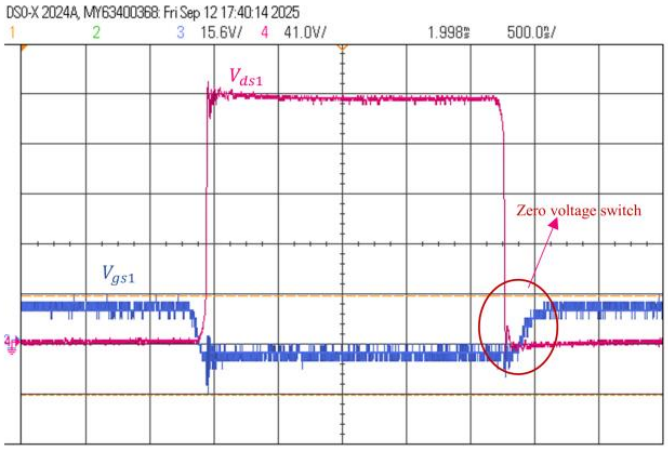

Figure 12 Experimental Results of Soft Switching

The red curve represents the waveform of the drain-source voltage V_{ds1} of the switching tube $S1$, and the blue curve represents the waveform of the gate-source voltage V_{gs1} of the switching tube $S1$. It can be observed from the figure that V_{ds1} has basically decreased to zero before its turn-on signal arrives, enabling ZVS operation of the switching tube and verifying the rationality of the resonant parameter calculation and device selection.

Due to the adoption of the IPOS topology and the unavoidable manufacturing tolerances of key passive components in the LLC resonant converter—such as the resonant inductor and resonant capacitor—the voltage balancing performance between the output phases imposes more stringent requirements. Any inter-phase voltage imbalance may result in uneven power distribution, which can further lead to increased device stress and degraded system reliability. Therefore, the output voltage balancing performance of the proposed converter was experimentally investigated in detail.

As shown in Figure 13, the two-phase output voltages were measured under full-load conditions with an input voltage of 200 V and an output voltage of 560 V. The experimental results indicate that the maximum voltage deviation between the two output phases is limited to 1.9%, demonstrating that the converter is capable of maintaining good output voltage balance even in the presence of component parameter dispersion. This result verifies the effectiveness of the adopted topology and control strategy in suppressing inter-phase imbalance, thereby ensuring stable and reliable operation of the system in high-power and high-voltage application scenarios.

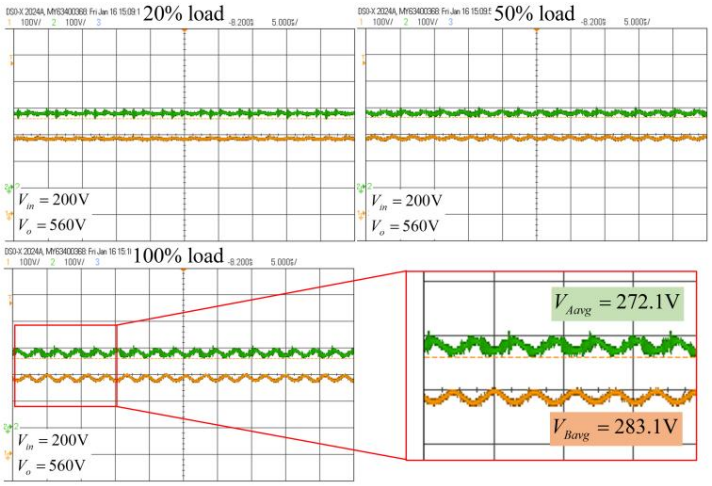

Figure 13 Output Voltage Balancing Waveforms Between Two Phases of the Prototype

Subsequently, the dynamic response characteristics and steady-state performance of the converter input current were experimentally verified under rated operating conditions, and the measured results are presented in Figure 13. During the experiments, step changes were applied to the input current reference through a host computer in order to emulate the operating conditions of a fuel cell system under load transients or operating-point transitions.

As can be observed from the experimental waveforms, when the input current reference is subjected to step changes with different amplitudes ranging from 20 A to 80 A, the actual input current of the converter is able to track the reference rapidly and accurately, without noticeable overshoot or oscillations. Throughout the entire dynamic regulation process, the system exhibits a smooth response with a short settling time, indicating that the proposed control strategy possesses excellent dynamic tracking performance.

Furthermore, after the completion of each step transition, the input current stabilizes around the target value with a small steady-state error. This demonstrates that the system maintains good steady-state control accuracy and operational

stability over a wide input current regulation range. The above experimental results confirm the converter's strong adaptability to input current variations under simulated fuel cell operating conditions, thereby providing experimental validation for its application in practical fuel cell energy conversion systems.

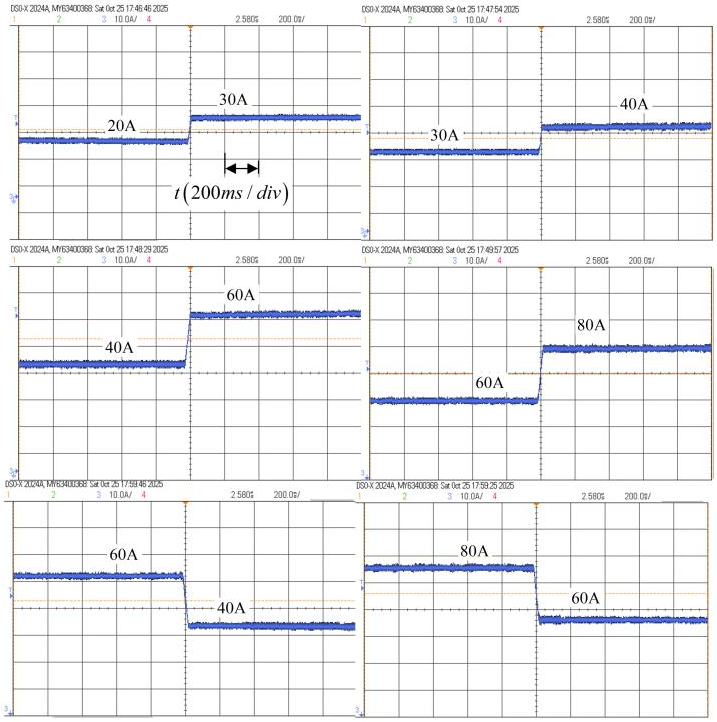

Figure 14 Experimental Results of Input Current Control

Finally, the overall energy conversion efficiency of the converter was experimentally evaluated under rated operating conditions, and the measured results are shown in Figure 14. During the experiments, the output voltage was maintained constant, while the input current was adjusted to assess the efficiency characteristics of the converter under different load levels.

As indicated by the experimental results, the converter efficiency initially increases rapidly with increasing input current and then gradually levels off. When the input current rises from 10 A to 30 A, the system efficiency improves from 91.2% to 95.5%, which is mainly attributed to the reduced proportion of fixed losses under higher load conditions. As the load continues to increase, the converter maintains a high efficiency level and reaches a peak efficiency of 96.6% at an input current of 70 A.

When the input current is further increased to 80 A and 90 A, a slight efficiency degradation is observed; however, the efficiency remains consistently above 96%. This indicates that the proposed converter exhibits excellent high-efficiency performance in operating regions close to the rated load. The above experimental results demonstrate that the designed LLC resonant converter achieves superior energy conversion performance under simulated fuel-cell operating conditions, satisfying the design requirements for high-efficiency and high-power-density applications (Figure 15).

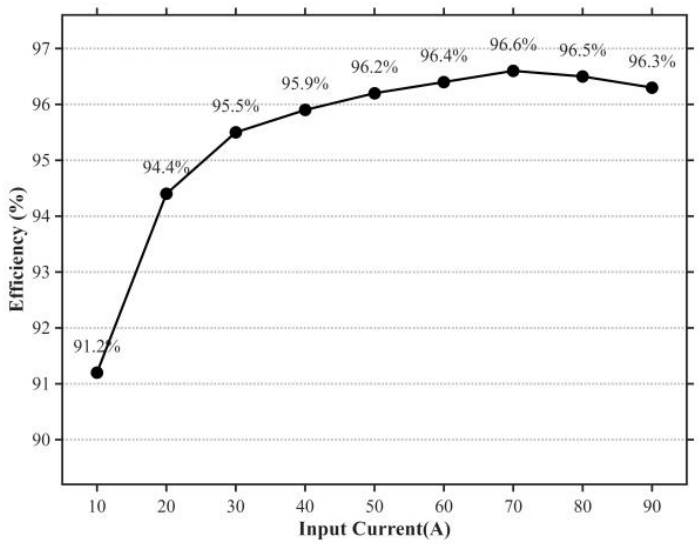

Figure 15 Experimental Results of Efficiency

5 CONCLUSION

This paper has presented an IPOS-type secondary LLC resonant DC–DC converter and a hybrid PFM–PSM control strategy for fuel-cell power conditioning applications requiring wide-range voltage regulation and high efficiency. By employing PFM as the primary modulation method and introducing a frequency-clamping with phase-shift compensation mechanism, the proposed control strategy effectively extends the controllable operating range under practical switching-frequency constraints while preserving soft-switching characteristics. The proposed converter and control approach were validated through both simulations and experimental tests on a laboratory prototype. Experimental results demonstrated a peak efficiency of 96.6% and efficiency above 96% near the rated load range. Meanwhile, good output voltage balancing was achieved with a maximum inter-phase deviation of 1.9% under full-load conditions, and fast, stable input-current tracking was observed under step reference changes. These results indicate that the proposed converter and hybrid control strategy provide a practical and effective solution for high-efficiency, wide-range fuel-cell energy conversion systems.

COMPETING INTERESTS

The authors have no relevant financial or non-financial interests to disclose.

REFERENCES

[1] Basha C H H, Mariprasath T, Murali M, et al. Simulative design and performance analysis of hybrid optimization technique for PEM fuel cell stack based EV application. Materials Today: Proceedings, 2022, 52: 290-295.
[2] Gunasekaran A, Sambasivam R, Ashokan A, et al. Realistic Simulation Analysis and Performance Testing Of One KW Fuel Cell Powered Three-Wheeler. Results in Engineering, 2025: 106336.
[3] Ramya V, Marimuthu R. A review on multi-input converters and their sources for fast charging of electric vehicles. Engineering Science and Technology, an International Journal, 2024, 57: 101802.
[4] Bairabathina S, Balamurugan S. Review on non-isolated multi-input step-up converters for grid-independent hybrid electric vehicles. International journal of hydrogen energy, 2020, 45(41): 21687-21713.
[5] Nie J, Meng L, Zhang H, et al. A three-level three-power-channel hybrid converter with wide voltage range for renewable energy medium voltage DC systems. Energy, 2025: 136940.
[6] Keerthi A, Dhanamjayulu C. A Thorough Review of Energy Management and an Advanced Control Techniques for Bi-directional DC-DC Converters in Electric Vehicle Applications. Results in Engineering, 2025: 106726.
[7] Abolghasemi M, Soltani I, Shivaie M, et al. Recent advances of step-up multi-stage DC-DC converters: A review on classifications, structures and grid applications. Energy Reports, 2025, 13: 3050-3081.
[8] El Hmidi J, Mansouri A, Ahaitouf A. Optimization approach of LLC resonant converter parameters for electric vehicles based on interior-point algorithm. Scientific African, 2025: e02939.
[9] Mahazabeen M, Abianeh A J, Ebrahimi S, et al. Enhancing ev charger resilience with reinforcement learning aided control. e-Prime-Advances in Electrical Engineering, Electronics and Energy, 2023, 5: 100276.
[10] Çelik Ö, Teke A, Tan A. Overview of micro-inverters as a challenging technology in photovoltaic applications. Renewable and Sustainable Energy Reviews, 2018, 82: 3191-3206.
[11] Wang D, Li N, Liu M, et al. Study on phase-shift value optimization strategy for extending soft-switching range of buck-boost LLC converters. Electric Power Systems Research, 2026, 251: 112250.
[12] Jingtao X, Guo X, Yao S. Coupled inductor integrated resonant converter with adaptive frequency control. Transactions of China Electrotechnical Society, 2023, 38(4): 998-1009.
[13] Li J, Qian T, Wang Y. A Three-port resonant converter with switches multiplexing and suppressed switching frequency range. IEEE Transactions on Circuits and Systems II: Express Briefs, 2023, 71(4): 2399-2403.
[14] Zhou Q, Liu B, Han M. Unified Modeling and Control Method of Hybrid Modulation of LLC Resonant Converter. In: Frontier Academic Forum of Electrical Engineering. Springer Nature Singapore, 2024: 22–33.
[15] Wang M, Pan S, Zha X, et al. Hybrid Control Strategy for An Integrated DAB-LLC-DCX DC-DC Converter to Achieve Full-Power-Range Zero-Voltage Switching, 2021.
[16] Liu Z, Chen W, Peng L, et al. An Improved IPOS LLC Resonant Converter With Sub-Module Output Voltage Sharing in Low Ripple High-Voltage Applications. IEEE Access, 2023, 11: 115316-115329.
[17] Zuo Y, Shen X, Du B, et al. Dual-mode Interleaved IPOS LLC Converter with 200-900V Output for EV DC Charging. IEEE Journal of Emerging and Selected Topics in Power Electronics, 2026.
[18] Wang F, Wang X, Ruan X. Model Building and Current Sharing Analysis for IPOP Converter System Based on Two-Stage LLC Resonant Converter//IECON 2023-49th Annual Conference of the IEEE Industrial Electronics Society. IEEE, 2023: 1-6.
[19] Liu K, Xiao T, Zhao J, et al. Differentiated-Gain-Regulation-Based Current Balancing Control for Multi-Phase Interleaved LLC Resonant Converters. IEEE Open Journal of Power Electronics, 2025.
[20] Zhang J, He Z, Han R, et al. Hybrid structure for an input-parallel output-serial DC-DC combined converter with high efficiency and high power density//2021 IEEE 12th Energy Conversion Congress & Exposition-Asia (ECCE-Asia). IEEE, 2021: 432-437.

[21] Liu W, Wang B, Yao W, et al. Steady-state analysis of the phase shift modulated LLC resonant converter//2016 IEEE Energy Conversion Congress and Exposition (ECCE). IEEE, 2016: 1-5.
[22] Alhatlani A, Ghosh S, Batarseh I. Comprehensive analysis and gain derivation of phase-shifted dual-input LLC converter. IEEE Access, 2022, 10: 116796-116807.